Deposition of Vanadium(V) Oxide Thin Films on Nitrogen-Containing Self-Assembled Monolayers†

Jing-Jong Shyue and Mark R. De Guire*

Department of Materials Science & Engineering, Case Western Reserve University, 10900 Euclid Avenue, Cleveland, Ohio 44106-7204

Received September 3, 2004. Revised Manuscript Received November 11, 2004

Vanadium oxide films have been deposited from aqueous solutions at low temperature on different self-assembled monolayer (SAM) modified silicon surfaces. Amine and ammonium salt SAMs were made via in situ transformations of bromide SAMs. The crystal structure and chemical composition of the vanadium oxide films were characterized by X-ray diffraction (XRD) and X-ray photoelectron spectroscopy (XPS). The films on alkylammonium salt SAMs were 3−4 times thicker than on amine SAMs under identical deposition conditions. In all cases, $V_2O_5 \cdot 1.6H_2O$ formed first (in the first 24 h), followed by $V_2O_5 \cdot H_2O$. The film growth rate showed two separate growth periods corresponding to the formation of these two phases. Mixed-valence and mixed-phase vanadium oxide films could be achieved by controlling the deposition conditions, whose effect on the kinetics of film growth has also been studied. Films up to 80 μm thick on alkylammonium salt SAM and 16 μm thick on amine SAM were grown in 72 h.

Introduction

As close-packed, highly ordered arrays of long-chain hydrocarbon molecules anchored to solid substrates,[1] self-assembled organic monolayers (SAMs) represent one type of organically functionalized surfaces that have been used to promote deposition of inorganic oxide and non-oxide thin films from aqueous media at low temperatures. (For a recent review, see ref 2.) Several studies have reported a dependence of film formation on the type of SAM surface functionality.[3−18] Recently, a general procedure of preparing SAMs with various surface functionalities from bromide SAMs was demonstrated.[19]

The chemistry of the precursors (reactant concentration, pH, temperature, type of metal salts, chelating agent, and method of solution preparation)[2,15,20−26] likewise affect the film's growth rate, microstructure, and properties. At the boundaries between the solid phase and the aqueous solution, even small changes in these parameters (especially concentration and pH) can result in different chemical composition or morphology of the product.

Vanadia-based materials have been chosen in this research because they have unusual physicochemical properties, making them useful as catalysts,[27] elements of switching devices,[28] photo- and electrochemical materials in information processing devices,[29] antistatic coatings,[30] sensors, reversible cathodes in lithium batteries,[31] and counter elec-

* To whom correspondence should be addressed. Telephone: (216) 368-4221. E-mail: mrd2@cwru.edu.

† Based in part on a thesis submitted for the M.S. degree in materials science and engineering of J.-J.S., Case Western Reserve University, 2002.

(1) Ulman, A. *Chem. Rev.* **1996**, *96*, 1533−1554.
(2) Niesen, T. P.; De Guire, M. R. *J. Electroceram.* **2001**, *6*, 169−207.
(3) Rieke, P. C.; Tarasevich, B. J.; Wood, L. L.; Engelhard, M. H.; Baer, D. R.; Fryxell, G. E. *Langmuir* **1994**, *10*, 619−622.
(4) Bunker, B. B.; Rieke, P. C.; Tarasevich, B. J.; Campbell, A. A.; Fryxell, G. E.; Graff, G. L.; Song, L.; Virden, J. W.; McVey, G. L. *Science* **1994**, *264*, 48−55.
(5) Shin, H.; Collins, R. J.; De Guire, M. R.; Heuer, A. H.; Sukenik, C. N. *J. Mater. Res.* **1995**, *10*, 699−703.
(6) Meldrum, F. C.; Flath, J.; Knoll, W. *Langmuir* **1997**, *13*, 2033−2049.
(7) Nagtegaal, M.; Stroeve, P.; Tremel, W. *Thin Solid Films* **1998**, *327−329*, 571−575.
(8) Nagtegaal, M.; Stroeve, P.; Ensling, J.; Gutlich, P.; Schurrer, M.; Voit, H.; Flath, J.; Kashammer, J.; Knoll, W.; Tremel, W. *Chem. Eur. J.* **1999**, *5*, 1331−1337.
(9) Meldrum, F. C.; Flath, J.; Knoll, W. *J. Mater. Chem.* **1999**, *9*, 711−724.
(10) Meldrum, F. C.; Flath, J.; Knoll, W. *Thin Solid Films* **1999**, *348*, 188−195.
(11) Koumoto, K.; Seo, S.; Sugiyama, T.; Seo, W. S. *Chem. Mater.* **1999**, *11*, 2305−2309.
(12) Aizenberg, J.; Black, A. J.; Whitesides, G. M. *J. Am. Chem. Soc.* **1999**, *121*, 4500−4509.
(13) Niesen, T. P.; Wolff, J.; Bill, J.; De Guire, M. R.; Aldinger, F. In *Organic−Inorganic Hybrid Materials II*; Klein, L. C., Francis, L. F., De Guire, M. R., Mark, J. E., Eds.; Materials Research Society: Warrendale, PA, 1999; Vol. 576, pp 197−202.
(14) Kovtyukhova, N. I.; Buzaneva, E. V.; Waraksa, C. C.; Martin, B. R.; Mallouk, T. E. *Chem. Mater.* **2000**, *12*, 383−389.
(15) Pizem, H.; Sukenik, C. N.; Sampathkumaran, U.; De Guire, M. R. *Chem. Mater.* **2002**, *14*, 2476−2485.
(16) Masuda, Y.; Wakamatsu, S.; Koumoto, K. *J. Eur. Ceram. Soc.* **2004**, *24*, 301−307.
(17) Masuda, Y.; Sugiyama, T.; Lin, H.; Seo, W. S.; Koumoto, K. *Thin Solid Films* **2001**, *382*, 153−157.
(18) Masuda, Y.; Saito, N.; Hoffmann, R.; De Guire, M. R.; Koumoto, K. *Sci. Technol. Adv. Mater.* **2003**, *4*, 461−467.
(19) Shyue, J.-J.; De Guire, M. R.; Nakanishi, T.; Masuda, Y.; Koumoto, K.; Sukenik, C. N. *Langmuir* **2004**, *20*, 8693−8698.
(20) Tarasevich, B. J.; Rieke, P. C.; Liu, J. *Chem. Mater.* **1996**, *8*, 292−300.
(21) Matijevic, E. *J. Colloid Interface Sci.* **1977**, *58*, 374−389.
(22) Matijevic, E. *Acc. Chem. Res.* **1981**, *14*, 22−29.
(23) Matijevic, E. *Annu. Rev. Mater. Sci.* **1985**, *15*, 483−516.
(24) Matijevic, E. *Pure Appl. Chem.* **1988**, *60*, 1479−1491.
(25) Matijevic, E. *Chem. Mater.* **1993**, *5*, 412−426.
(26) Livage, J.; Henry, M.; Sanchez, C. *Prog. Solid State Chem.* **1988**, *18*, 259−341.
(27) Petrov, L. A.; Lobanova, N. P.; Volkov, V. L.; Zakharova, G. C.; Kolenko, I. P.; Bulkakova, L. J.; Akademii, I. *Khimicheskaya* **1989**, *9*, 1967.
(28) Bullot, J.; Gallais, O.; Gauthier, M.; Livage, J. *Appl. Phys. Lett.* **1980**, *36*, 986−988.
(29) Morineau, R.; Chemseddine, A.; Livage, J. Fr. Patent 208,934, 1983.
(30) Livage, J.; Beteille, F.; C., R.; Chatry, M.; Davidson, P. *Acta Mater.* **1998**, *46*, 743−750.

10.1021/cm048501x CCC: $30.25 © 2005 American Chemical Society
Published on Web 01/14/2005

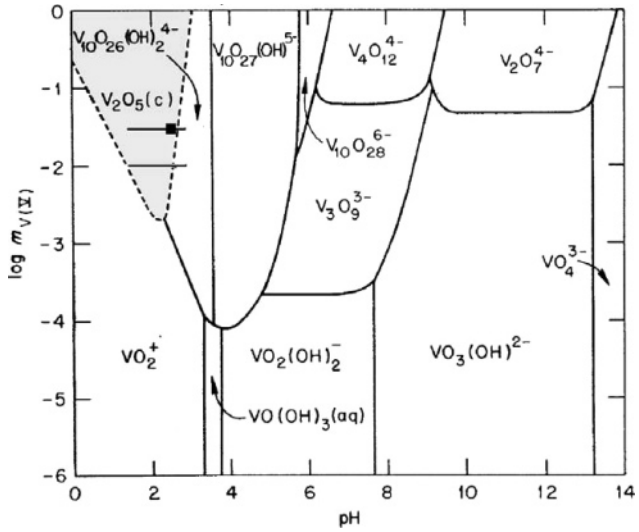

Figure 1. Predominance diagram of $V^{(V)}-OH^-$ under 25 °C with ionic strength of 1 *m* as a function of vanadium concentration $m_{V(V)}$ and pH [Adapted from Baes, C. F., Jr.; Mesmer, R. E. *The Hydrolysis of Cations*; Robert E. Krieger Publishing Company, Inc.: Malabar, FL, 1976.] Horizontal lines in the shaded region indicate conditions studied here, though at higher temperature.

trodes in electrochromic display devices.[31] Vanadium oxide films are also known to exhibit both electronic and ionic conduction.[31] Some of these applications (such as catalysis and antistatic coatings) utilize vanadium oxide in one or more of its hydrated forms, such as those found in the films described in the present work. Therefore, a deposition process that yields such films via simple aqueous chemistry under near-ambient conditions without subsequent heat treatment may have significant technological interest.

Figure 1[32] shows the predominance diagram of the vanadium(V) oxide−hydrate system. (Due to the lack of thermodynamic data, a predominance map for temperatures other than 25 °C has not been determined.) For the present work, the critical boundary between solid and aqueous phases studied here is the one between $[V_{10}O_{26}(OH)_2]^{4-}$ and V_2O_5(s). The growth mechanism of vanadia is known to proceed from small oligomers to higher polymers to colloids.[33] Therefore, the desired starting species would be $[V_{10}O_{26}(OH)_2]^{4-}$ (oligomer) instead of VO_2^+ (monomer).

Experimental Procedures

General. X-ray photoelectron spectroscopic (XPS) peak positions are reported in units of electrovolts in binding energy and were recorded on a PHI Model 5600 MultiTechnique system. XPS peaks are referenced to the Si 2p peak of single-crystal (100) silicon at 99.7 eV. Scanning electron microscopic (SEM) images were taken with a Hitachi S-4500 or Philips XL30 system using a secondary electron (SE) detector. The thicknesses of the films were measured directly from SEM images of cross-sectional fracture surfaces. The X-ray diffraction (XRD) patterns are reported in units of degrees (2θ) and were recorded at grazing incidence on a Scintag Advanced Diffraction System with Cu Kα X-ray source while fixing the X-ray source at 1° with 0° sample tilt and varying the angle of the detector.

The preparation of SAMs-modified Si single crystal substrates with amine ($-NH_2$) and alkylammonium ($-N^+(CH_3)_3$) surface functionalities was identical to that reported previously.[19] The only difference is that a surfactant with a 16-carbon chain (1-bromo-16-(trichlorosilyl)hexadecane) was used here.

Stock Deposition Solution. Following Niesen,[13,34] ammonium metavanadate NH_4VO_3 (0.585 g, 5 mmol) was dissolved in 50 mL of distilled water at 80 °C. This solution was passed through Amberlite IR-120 proton exchange resin. To adjust the pH to desired values between 1.2 and 3.0, 10% HCl was added dropwise. The resulting solution was diluted with degassed distilled water to 200 or 500 mL to prepare 25 or 10 mN $[V_{10}O_{26}(OH)_2]^{4-}$ solution.

Observation of Induction Times (t_{ind1}, t_{ind2}). Aliquots (20 mL each) of vanadium solution were put in sealed tubes and placed in an oil bath at 45, 65, or 85 °C. The tubes were observed at 10-min intervals. The times for first appearance of scattering (t_{ind1}) of a 635 nm, 5 mW laser beam from a laser pointer and for first appearance of turbidity visible to the naked eye (t_{ind2}) were recorded over a period of 24 h. The pH value was then recorded.

Thermodynamic Calculation of $V^{(V)}O_2^+-[V^{(V)}_{10}O_{26}(OH)_2]^{4-}-V^{(IV)}O^{2+}-H^+-V_2O_5$(s) Equilibrium. Published thermodynamic data for the vanadium system were used to calculate the equilibrium pH values for the present solutions at the temperatures of interest. The following assumptions were made:

(1) The activity coefficient of all species is 1.

(2) The activity of water is 1 and the pressure of oxygen is 0.2 atm.

(3) Values of ΔG for the solution equilibria do not change with temperature.

Calculations were performed with a C++ program as described in the Supporting Information.

Results and Discussion

Solution Chemistry. One of the equilibria between vanadium and water is represented by

$$10V^{(V)}O_2^+ + 8H_2O \rightleftharpoons 14H^+ + [V^{(V)}_{10}O_{26}(OH)_2]^{4-} \qquad \Delta G = 55\ \text{kJ} \quad (1)$$

It is known that color identifies the major species in aqueous vanadium solutions: VO_2^+ is bright orange (appears at low pH), while $[V_{10}O_{26}(OH)_2]^{4-}$ is duller orange (appears at slightly higher pH) at any given concentration.[35] For the present solutions at 25 °C, this crossover occurred at $1.47 < pH < 1.68$ at 10 mN vanadium and at $1.42 < pH < 1.82$ at 25 mN vanadium.

When solid formed, many of the solutions self-adjusted their pH to a value near 2.5, implying that a common equilibrium solution concentration was being reached in these cases (Tables 1 and 2). To model the conditions involving precipitation requires introducing equilibria involving solid V_2O_5. As indicated in Figure 1, $[V^{(V)}_{10}O_{26}(OH)_2]^{4-}$ is the dominant species in equilibrium with V_2O_5 at higher pH:[32]

$$[V^{(V)}_{10}O_{26}(OH)_2]^{4-} + 4H^+ \rightleftharpoons 3H_2O + 5V_2O_5(s) \qquad \Delta G = -9\ \text{kJ} \quad (2)$$

(31) Livage, J. *Chem. Mater.* **1991**, *3*, 578−593.
(32) Baes, C. F. J.; Mesmer, R. E. In *The Hydrolysis of Cations*; Robert E. Krieger Publishing Company, Inc.: Malabar, FL, 1976; pp 197−210.
(33) Von Hhosh, S.; Dhar, N. R. *Anorg. Chem.* **1930**, *190*, 421.
(34) Niesen, T. P.; Wolff, J.; Bill, J.; Wagner, T.; Aldinger, F. In *Ninth CIMTEC World Forum on New Materials*; Vincenzini, P., Ed.; Techna Srl: Faenza, 1999; pp 27−34.
(35) Greenwood, N. N.; Earnshaw, A. *Chemistry of the Elements, 2nd ed.*; Reed Educational and Professional Publishing Ltd.: Woburn, MA, 1997; pp 976−999.

Table 1. Induction Times for Laser Scattering (t_{ind1}) and Visible Turbidity (t_{ind2}) for 10 mN Vanadium Solutions at Different Temperatures and pH Values

initial pH, 25 °C	1.27	1.47	1.68	1.92	2.11	2.35	2.44	2.68	2.91
color	bright orange	bright orange	orange	orange	orange	orange	orange	orange	orange
85 °C, t_{ind1} (h)	*b*	*b*	0.5	0.5	0.5	0.67	2.5	*b*	b
85 °C, t_{ind2} (h)	*b*	*b*	1.5	1.5	1.5	2.5	4	~16[a]	*b*
color	*b*	*b*	red gel	brown gel	brown gel	brown gel	brown gel	yellow particle	*b*
final pH (24 h)	1.27	1.47	2.2	2.23	2.25	2.28	2.31	2.48	2.91
65 °C, t_{ind1} (h)	*b*	*b*	2.5	2	2	3	*b*	*b*	*b*
65 °C, t_{ind2} (h)	*b*	*b*	3	2.5	2.5	5	~16[a]	*b*	*b*
color	*b*	*b*	brown gel	brown gel	brown gel	brown gel	yellow particle	*b*	*b*
final pH (24 h)	1.27	1.47	2.21	2.22	2.26	2.35	2.38	*2.68*	*2.91*
45 °C, t_{ind1} (h)	*b*	*b*	*b*	*b*	*b*	*b*	*b*	*b*	*b*
45 °C, t_{ind2} (h)	*b*	*b*	~16[a]	~16[a]	~16[a]	~16[a]	*b*	*b*	*b*
color	*b*	*b*	yellow particle	yellow particle	yellow particle	yellow particle	*b*	*b*	*b*
final pH (24 h)	1.27	1.47	2.19	2.25	2.24	2.32	2.44	2.68	2.91

[a] Nothing happened in first 5 h, but precipitation occurred after 16 h. [b] Unchanged after 24 h.

Table 2. Induction Times for Laser Scattering (t_{ind1}) and Visible Turbidity (t_{ind2}) for 25 mN Vanadium Solutions at Different Temperatures and pH Values

initial pH, 25 °C	1.39	1.42	1.84	1.81	1.91	2.38	2.47	2.68	2.86
color	bright orange	bright orange	orange	orange	orange	orange	orange	orange	orange
85 °C, t_{ind1} (h)	*b*	*b*	0.17	0.17	0.17	0.17	0.17	0.25	0.33
85 °C, t_{ind2} (h)	*b*	*b*	0.33	0.33	0.33	0.33	0.33	0.67	2.50
color			red gel	red gel	red gel	brown gel	brown gel	yellow particle	yellow particle
final pH (24 h)	1.39	1.42	2.48	2.47	2.5	2.51	2.55	2.64	2.85
65 °C, t_{ind1} (h)	*b*	*b*	0.25	0.25	0.25	0.25	0.25	2	2.5
65 °C, t_{ind2} (h)	*b*	*b*	0.5	0.5	0.5	0.5	0.5	3	3.5
color			red gel	red gel	red gel	brown gel	brown gel	yellow particle	yellow particle
final pH (24 h)	1.39	1.42	2.21	2.51	2.49	2.46	2.48	2.67	2.88
45 °C, t_{ind1} (h)	*b*	*b*	1	1	1	1	1	3	a
45 °C, t_{ind2} (h)	*b*	*b*	2.5	2.5	2.5	2.5	2.5	5	17
color			red gel	red gel	brown gel	brown gel	brown gel	yellow particle	yellow particle
final pH (24 h)	1.39	1.42	2.25	2.43	2.48	2.41	2.46	2.63	2.87

[a] Laser scattering was not observed. [b] Unchanged after 24 h.

At lower pH, the dominant species in equilibrium with V_2O_5 is $V^{(V)}O_2^+$:[32]

$$V^{(V)}O_2^+ + (1/2)H_2O \rightleftharpoons H^+ + (1/2)V_2O_5(s) \qquad \Delta G = -3.8 \text{ kJ} \quad (3)$$

When solid vanadia is present, at equilibrium the pH will stabilize at a value that satisfies eqs 1−3 simultaneously. The calculated equilibrium pH ranges from 3.3 at 25 °C to 2.8 at 85 °C for initial pH values above 2.5, within 0.1−0.6 pH unit of the "final pH" values reported in Table 1. (Details of these calculations are provided in the Supporting Information.)

It is known that additional equilibria involving the reduction of some vanadium(V) to vanadium(IV) are significant during the synthesis of vanadia[31] (eqs 4 and 5[32]):

$$2[V^{(V)}{}_{10}O_{26}(OH)_2]^{4-} + 48H^+ \rightleftharpoons 5O_2 + 26H_2O + 20V^{(IV)}O^{2+} \qquad \Delta G = 330 \text{ kJ} \quad (4)$$

$$V^{(V)}O_2^+ + H^+ \rightleftharpoons (1/4)O_2 + (1/2)H_2O + V^{(IV)}O^{2+} \qquad \Delta G = 22 \text{ kJ} \quad (5)$$

When these equilibria are considered, it can be shown (see the Supporting Information for details) that the equilibrium ratio of vanadium(IV) in the solution increases rapidly for initial pH lower than 2.5 for 10 mN vanadium and lower than 2.2 for 25 mN vanadium. Some of these reduced $V^{(IV)}$ species apparently can become incorporated into the solid phase and thus are responsible for the reported mixed-valence character of vanadium oxide gels.[36] The amount of $V^{(IV)}$ ions in solution is usually less than about 1%. (It can be as high as 10%[37] to 20%[38] when synthesis is in an organic solution, because $V^{(V)}$ is easier to reduce in organic solvents.) In the present work, no crystalline phases containing $V^{(IV)}$ were detected in films formed from solutions with initial pH of either 2.9 or 2.5. XPS detected only $V^{(V)}$ in the films (Figure 2, left), except in a film deposited at initial pH of 1.8, which showed significant broadening of the V_{2p3} peak, consistent with the presence of vanadium(IV) and/or vanadium(III) (Figure 2, right). The curve fitting suggests that 40% of the vanadium in the surface of this film was V^{4+}.

V(IV) species also play an important role in the formation of V_2O_5 gels by acting as polymerization initiators.[36,39] The suggested mechanism is that the larger $V^{(IV)}$ ion favors coordination expansion,[40] and promotes the formation of condensed species from tetrahedrally coordinated to octahedrally coordinated species[30] by acting as a bridge between two $V^{(V)}$ complexes. Therefore, solutions with lower initial pH (and therefore higher $V^{(IV)}$ concentrations) could give

(36) Gharbi, N.; Sanchez, C.; Livage, J.; Lemerle, J.; Nejem, L.; Lefebvre, J. *Inorg. Chem.* **1982**, *21*, 2758−2765.
(37) Hioki, S.; Ohishi, T.; Takahashi, K.; Nakazawa, T. *J. Ceram. Soc. Jpn., Int. Ed.* **1989**, *97*, 617.
(38) Babonneau, F.; Barboux, P.; Josien, F. A.; Livage, J. *J. Chim. Phys.* **1985**, *82*, 761.
(39) Lemerle, J.; Nejem, L.; Lefebvre, J. *J. Inorg. Nucl. Chem.* **1980**, *42*, 17.
(40) Nabavi, M.; Sanchez, C. C. *Acad. Sci. Paris* **1990**, *310*, 117.

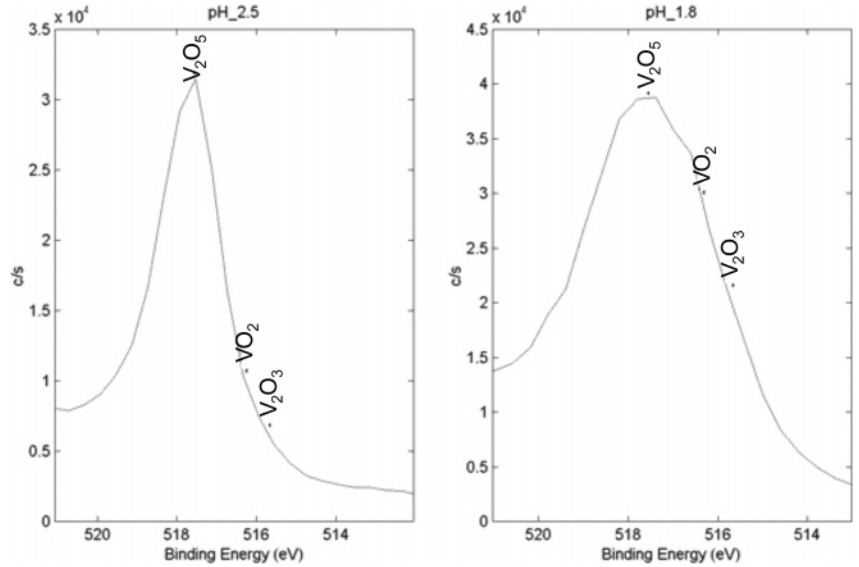

Figure 2. XPS V_{2p3} signal of vanadia films formed from solutions with 25 mN vanadium, 45 °C, and initial pH 2.5 (left) and pH 1.8 (right). Positions for different valences of vanadium are marked.

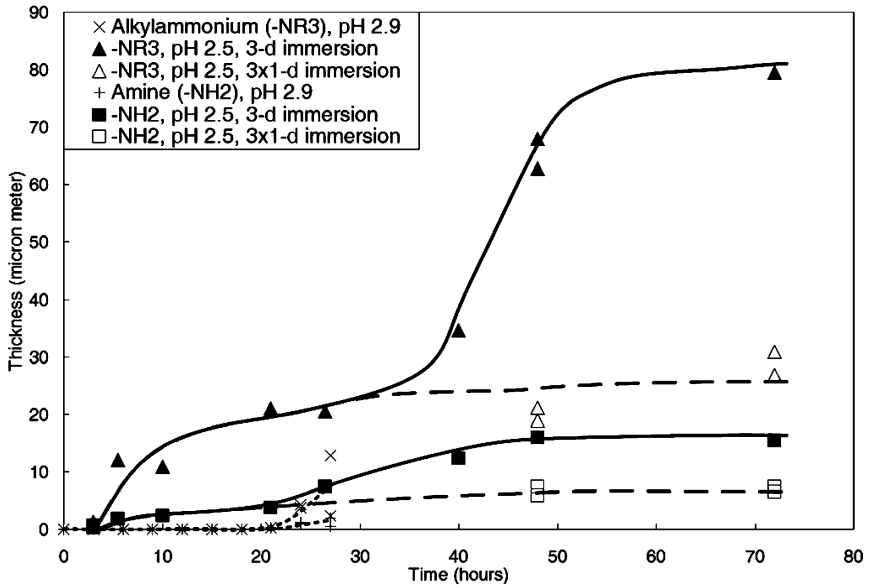

Figure 3. Growth kinetics of vanadium oxide films under different conditions on different SAMs. Concentration of vanadium was 25 mN at 45 °C.

faster precipitation. The observed induction times for laser scattering (Tables 1 and 2) reflect this behavior, with t_{ind} decreasing as pH decreased on crossing from the $[V^{(V)}{}_{10}O_{26}(OH)_2]^{4-}$ side of the diagram.

Effect of Solution Conditions on Growth Rate of Vanadia Films. Depositions carried out at 45 °C with an initial pH of 2.5 and vanadium concentration of 25 mN gave a short induction time, a stable colloidal suspension in the solution, and no signs of $V^{(IV)}$. The same conditions except with pH 2.9 (i.e., unaltered by adding HCl) were used as an untuned reference condition.

Figure 3 shows the growth of vanadium oxide films at these two initial pH values on two different types of SAM. There was no evidence of film formation (cf. Table 2) at pH 2.9 before 17 h and at pH 2.5 before 3 h. This could be understood in terms of the concentration of $V^{(IV)}$ species, which are known as polymerization initiators[36,39] for the formation of vanadia. These would be discouraged from forming at the higher pH (2.9). As a result, it took a much longer time to achieve a certain sufficient $V^{(IV)}$ concentration in order to initiate the film formation. As with previous observations of ZrO_2 films, no film formation occurred before the induction time (cf. Tables 1 and 2) was complete[41] nor on bare hydrolyzed silicon.[42] Therefore, it is presumable that the films grew via attachment of particles nucleated in the bulk solution, and that the substantial positive zeta potentials of amine (~75 mV at pH 3)[19] and alkylammonium SAMs (~105 mV at pH 3)[19] played a role in assembling the particles into the observed films. (As reported in ref 19, the bare silicon exhibits weak positive zeta potential, ~30 mV at pH 3.)

It is noteworthy that the films on alkylammonium SAMs were much thicker (~3 times) than on amine SAMs under

(41) Agarwal, M.; De Guire, M. R.; Heuer, A. H. *J. Am. Ceram. Soc.* **1997**, *80*, 2967−2981.
(42) Shyue, J.-J.; De Guire, M. R. In *CIMTEC 2002 (10th International Ceramics Congress and 3rd Forum on New Materials)*; Vincenzini, P., Ed.; Florence, Italy, 2002; Techna Srl: Faenza, p 469−480.

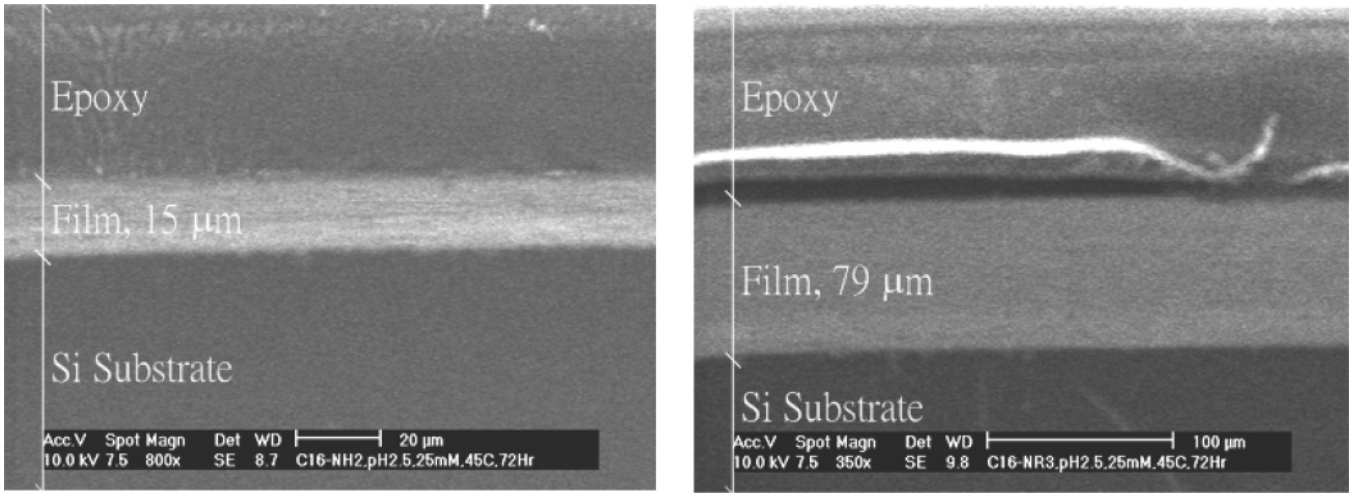

Figure 4. Cross section of vanadium deposited with 25 mN vanadium, pH 2.5, 45 °C, 3 days on amine (left) and alkylammonium (right) surfaces.

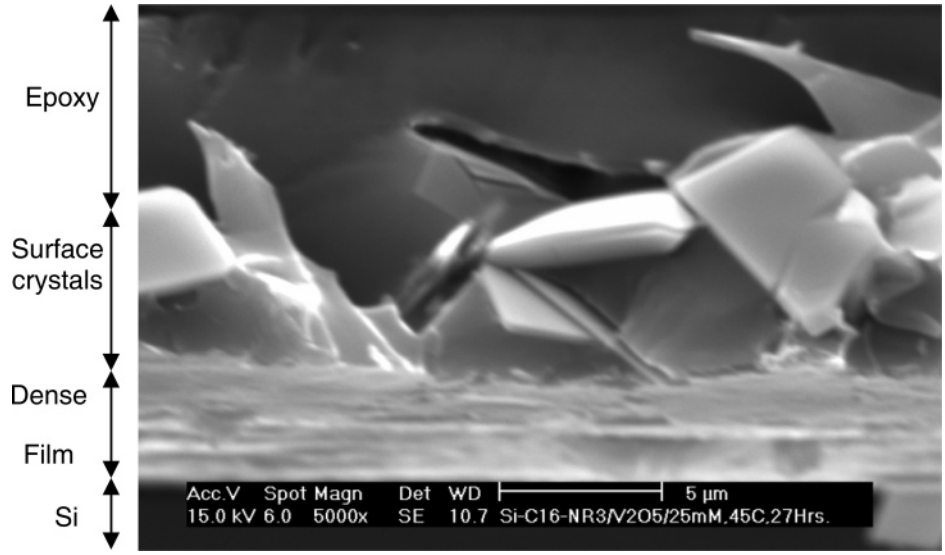

Figure 5. Vanadium oxide film on alkylammonium salt SAM coated surface. The deposition conditions were 25 mN vanadium, pH 2.9, 45 °C, 27 h. Note: the surface crystals were not counted in the film thickness.

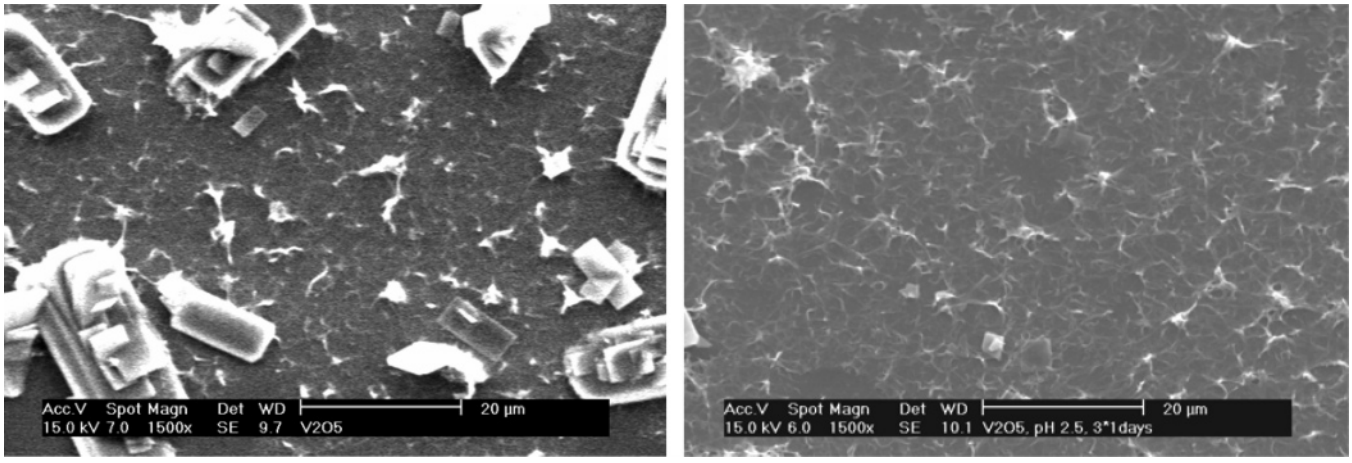

Figure 6. Topography of vanadia films deposited under 25 mN vanadium, 45 °C, pH 2.9, 27 h (left), and pH 2.5, 72 h (right).

identical deposition conditions.[42] Under these conditions, amine SAMs are reported to be ∼40% protonated (i.e., positively charged),[19] and their zeta potential is ∼30% lower than that of alkylammonium SAMs.[19] These surfaces also exhibit forces toward oxide particles that scale with the degree of charge on the respective surfaces.[43] Therefore, it is clear that the alkylammonium SAMs possess much stronger positive surface charge than the amine SAMs. Because vanadia particles formed in the deposition solution should be slightly negatively charged at the pH studied (pH >2.5), the electrostatic interaction should be much stronger on the alkylammonium SAMs. How this electrostatic dif-

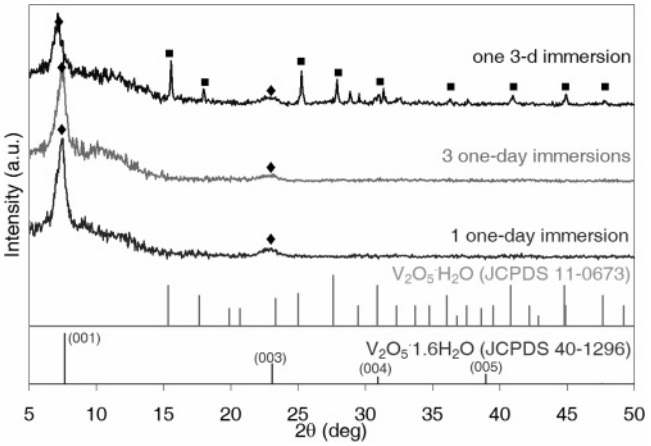

Figure 7. XRD of vanadia films formed from solutions with pH 2.5, 45 °C, 25 mN vanadium, using different types of immersion. ■, $V_2O_5·H_2O$; ◆, $V_2O_5·1.6H_2O$.

ference can exert effects on the growth rates of films at the micrometer scale is not well understood. Nevertheless, similar long-range effects apparently attributable to surface charge differences have been observed with titania films on sulfonate and amine SAMs and bare silicon,[43,44] with titania−vanadia films on sulfonate and carboxylate SAMs,[45] with tin oxide films on sulfonate SAMs and bare silicon,[46] and with hydroxyapatite on amine SAMs and hydrolyzed silicon.[47]

The films deposited for 3 days at pH 2.5 were dense on both types of SAM (Figure 4), while the film deposited at pH 2.9 consisted of large crystals on a dense inner film (Figure 5) after deposition for 27 h, leading to a significantly rougher surface. This is consistent with the fact that, at high pH, vanadium oxide tends to form a few large crystals rather than a colloid gel: at pH 2.9, laser scattering was not observed, and a solid phase settled after 17 h. This result suggests that the dense, inner film was grown via nucleation on the substrate instead of particle attachment, since the dense inner film grew to a thickness of a few micrometers even though colloid formation was not observed at pH 2.9 (Table 1).

Due to the formation of surface crystals at an initial pH 2.9 after 27 h, the topography was quite different between these two deposition conditions (Figure 6). Many bulky surface crystals formed on top of the dense vanadia film after 27 h at pH 2.9. However, at pH 2.5, even after 3 days there were just a few small surface crystals, while overall the films were dense, uniform, and fine-grained.

It should be noted that the final film thicknesses observed here (5−80 μm, Figure 3), as well as the average growth rates (up to 1 μm h^{-1}), are unusually high for simple oxide films deposited on SAMs from aqueous media, which usually exhibit maximum thicknesses <1 μm and maximum growth

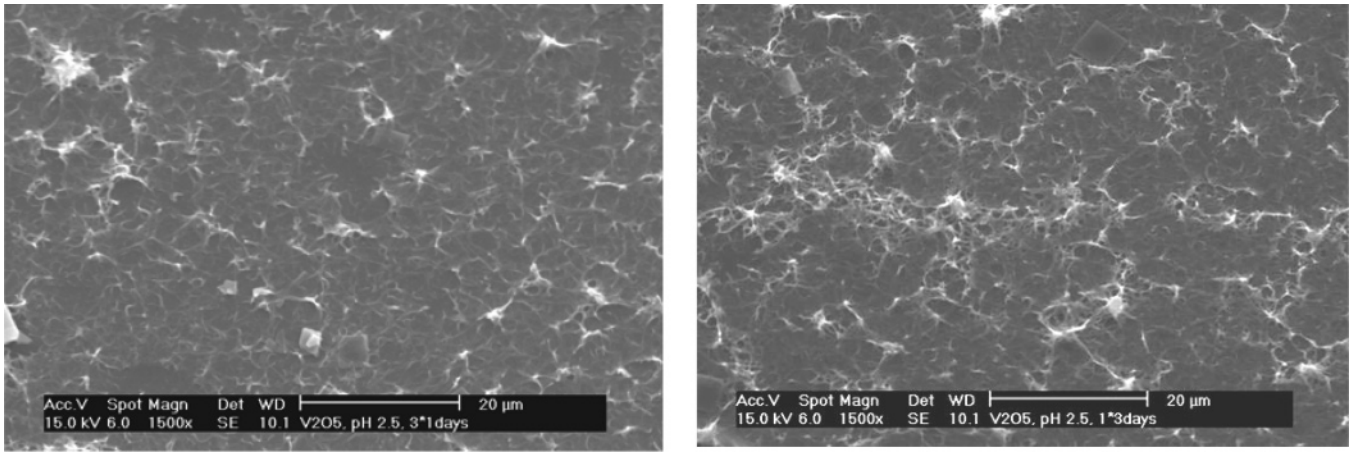

Figure 8. Topography of vanadium oxide films at pH 2.5, 25 mN vanadium, 45 °C, using one 3-day immersion (left) and three 1-day immersions in fresh solution (right).

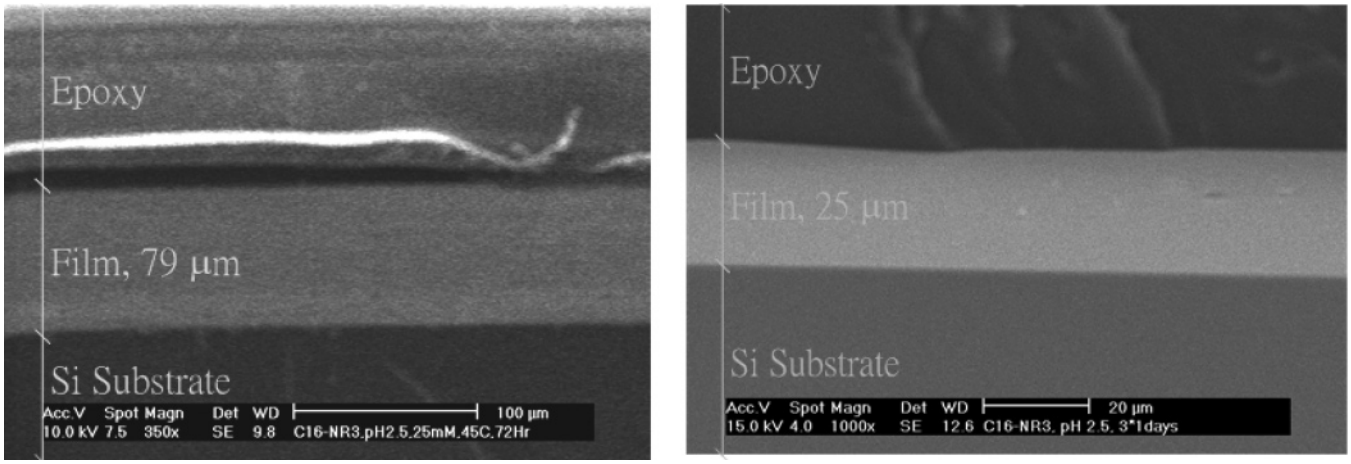

Figure 9. Cross section of vanadium oxide films at pH 2.5, 25 mN vanadium, 45 °C, using one solution for 3 days (left) and using fresh deposition three times, 24 h each.

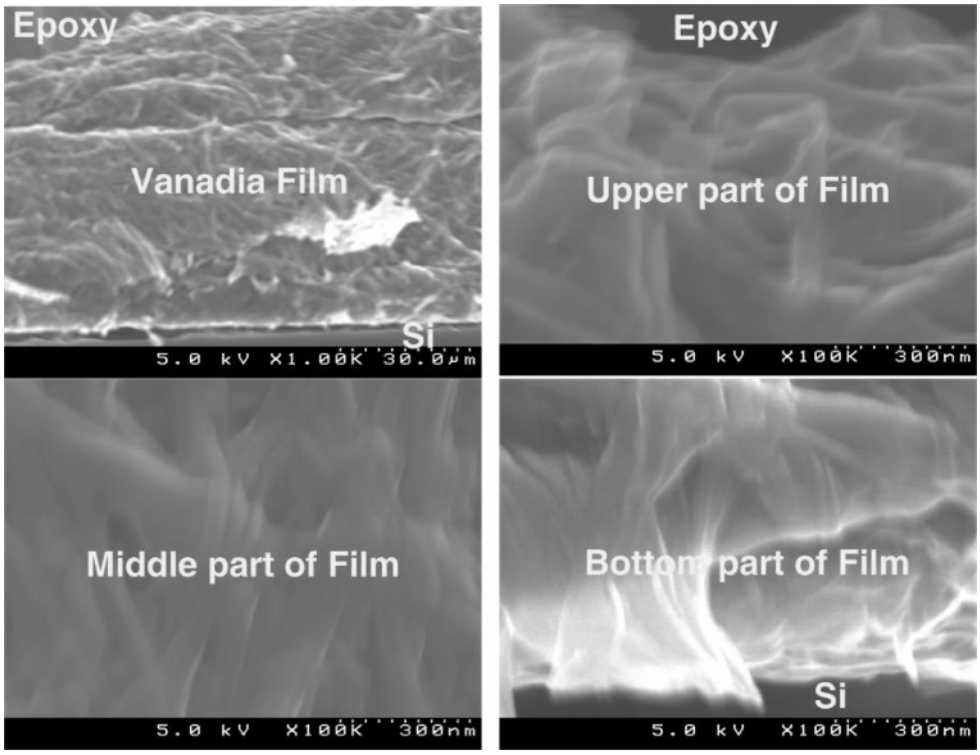

Figure 10. Cross section of different regions of vanadium oxide films formed on alkylammonium salt SAMs with 25 mN vanadium, 45 °C, pH 2.5, 72-h single immersion. Although different phases were observed with the XRD during different stages of film growth, no microstructural difference was observed here.

rates of tens of nannometers per hour.[2,15] The ability of these hydrated vanadia phases to grow much more quickly than other oxides (titania, zirconia, tin oxide) may be attributable to their highly layered crystal structure and growth habit (see below).

Crystallography and Microstructure of Vanadium Oxide Films. At pH 2.5, the growth rates on both amine and alkylammonium SAMs showed two-step growth kinetics (Figure 3). Films grown for longer than 24 h showed a second phase in XRD, $V_2O_5 \cdot H_2O$, in addition to the $V_2O_5 \cdot 1.6H_2O$ that formed at shorter times.

To try to isolate these two apparent stages of growth, films were grown by changing the solution every 24 h to a total deposition time of 3 days. The resulting XRD patterns are shown in Figure 7. (The broad hump around 12° is from the sample holder.)

After 3 days in the same solution, the monohydrate $V_2O_5 \cdot H_2O$ dominates the pattern, indicating that it is the major phase in the top 50 μm of the film. The pattern for the 3 × 1-day film clearly shows that the monohydrate phase was not present, and the two-step growth kinetics seen in the single 3-day immersion were not observed. Therefore, it can be concluded that the second growth plateau seen in Figure 3 is due to the deposition of $V_2O_5 \cdot H_2O$. The monohydrate apparently has a longer induction time than does $V_2O_5 \cdot 1.6H_2O$ but a faster growth rate once it forms. The average thickness of the crystals, estimated using the Scherrer equation, was 10−12 nm for $V_2O_5 \cdot 1.6H_2O$ and 53−54 nm for $V_2O_5 \cdot H_2O$. The appearance of only 00*l* peaks in the XRD pattern of $V_2O_5 \cdot 1.6H_2O$ indicates the high degree of orientation (*c*-axis perpendicular, and V−O layers parallel, to the substrate) exhibited by this phase in the present films.

Microstructural investigation of these films in plan view (Figure 8) and in cross section (Figures 9 and 10) showed a characteristic "wrinkled" morphology reported by Niesen et al.[13,34] The features shown in high-resolution FE-SEM (Figure 10) are the trace of the fibrous structure shown in Figure 8.

No features were observed that distinguished $V_2O_5 \cdot H_2O$ from $V_2O_5 \cdot 1.6H_2O$. This can be explained in terms of the nature of the crystal structure of vanadium oxide hydrate. The *c* lattice parameter varies from 8.75 Å for $V_2O_5 \cdot 0.5H_2O$ (JCPDS 40-1297) to 12.25 Å for $V_2O_5 \cdot 3H_2O$ (JCPDS 07-0332). This corresponds to progressive intercalation of water between the layers of V−O square pyramid networks, expanding the *c*-axis perpendicular to the layers with essentially no change in the structure of the layers themselves. Therefore no conspicuous differences in growth habit between the two phases are expected.

Quality of Vanadia Films. If the deposition solution was degassed properly and did not form bubbles during deposition, films thicker than 10 μm on either amine or alkylammonium salt SAMs at pH 2.5 exhibited no notable cracks or pinholes, as indicated by the absence of silicon peaks in XPS and SEM topography (Figure 8). The absence of cracks in films this thick is notable: Pizem et al.[15] reported that titania films thicker than ~300 nm deposited from aqueous

(43) Shyue, J.-J.; Tang, Y.; De Guire, M. R. *J. Mater. Chem.* **2005**, *15*, 323−330.
(44) Niesen, T. P.; Bill, J.; Aldinger, F. *Chem. Mater.* **2001**, *13*, 1552−1559.
(45) Shyue, J.-J.; De Guire, M. R. *Trans. MRS-J* **2004**, *29*, 2383−2386.
(46) Supothina, S.; De Guire, M. R.; Heuer, A. H. *J. Am. Ceram. Soc.* **2003**, *86*, 2074−2081.
(47) Zhu, P.; Masuda, Y.; Koumoto, K. *J. Colloid Interface Sci.* **2001**, *243*, 31−36.

solutions on SAMs exhibited drying cracks. The absence of cracks in the present films may be a consequence of the layered crystal structure of the hydrated vanadia phases and the high degree of *c*-axis texturing exhibited by the $V_2O_5 \cdot 1.6H_2O$ phase. As discussed above, loss of water of crystallization results in contraction of the *c*-axis, with little change in the atomic arrangements in the V−O layers themselves. On the microstructural scale, for layers oriented with their *c*-axis perpendicular to the substrate, the volume change associated with this water loss will be accommodated primarily by a reduction in film thickness, with little dimensional change parallel to the V−O layers to generate the in-plane stresses that cause cracks.

All the films survived ultrasonic agitation for 20 min in absolute ethanol, indicating that they are adherent to the substrate. However, using a simple tape-peel test with Scotch tape on an 80 μm thick vanadium oxide film on alkylammonium salt SAM, XPS showed that part of the film was removed from the specimen. This indicates that the strength within the film itself was not high, probably due to the weak hydrogen bonding between layers. Nevertheless, the substrate coverage remained 100%, since no silicon signal from the substrate could be detected using XPS.

Conclusion

The deposition conditions of hydrated vanadium oxide on amine and alkylammonium salt SAMs were studied. Dense films up to 3 μm thick formed in less than 24 h apparently by nucleation on the substrate, as no precipitation was observed in the solution. At pH 2.9 after 24 h, large crystals formed on the dense films and the roughness increased significantly. This was found to be consistent with slow nucleation kinetics at this pH, as observed in studies of the induction time. Vanadium was pentavalent in these films, whereas at pH 1.8 mixed-valence (V^{4+} and V^{5+}) vanadium oxide films were deposited, as shown by XPS.

The deposition condition studied most extensively here was at pH 2.5, which appears to be the best condition for making uniform, dense, thick (up to 80 μm), and single-valence (to the limits of XPS, 0.1%) vanadium(V) oxide film in relatively short times. However, mixed vanadium oxide hydrate phases formed if the deposition solution was more than 24 h old. This mixed-phase film ($V_2O_5 \cdot H_2O$ and $V_2O_5 \cdot 1.6H_2O$) can be avoided by changing the deposition every 24 h, during which time only $V_2O_5 \cdot 1.6H_2O$ formed.

In single 72-h depositions, mixed-phase vanadium oxide films ($V_2O_5 \cdot H_2O$ and $V_2O_5 \cdot 1.6H_2O$) up to 80 μm thick were formed on alkylammonium salt SAMs, and about 16 μm thick on amine SAMs. Using three consecutive 24-h depositions in fresh solutions, single-phase vanadium oxide films ($V_2O_5 \cdot 1.6H_2O$) up to 30 μm thick were formed on alkylammonium SAMs, while films about 7 μm thick formed on amine SAMs.

Acknowledgment. Sponsorship of the US National Science Foundation through Grants DMR 9803851 and DMR 0203655 is gratefully acknowledged.

Supporting Information Available: Thermodynamic calculation of $V^{(V)}O_2^+ - [V_{10}O_{26}(OH)_2]^{4-} - V^{(IV)}O^{2+} - H^+$ equilibrium, XPS spectrum after tape-peel test, source code of the computer program (PDF). This material is available free of charge via the Internet at http://pubs.acs.org.

CM048501X